Accelerated Publications

Three-Dimensional Structure of DesVI from *Streptomyces venezuelae*: A Sugar *N*,*N*-Dimethyltransferase Required for dTDP-Desosamine Biosynthesis[†,‡]

E. Sethe Burgie and Hazel M. Holden*

Department of Biochemistry, University of Wisconsin, Madison, Wisconsin 53706

Received January 11, 2008; Revised Manuscript Received January 31, 2008

ABSTRACT: D-Desosamine, or 3-(dimethylamino)-3,4,6-trideoxyglucose, is an unusual sugar found on the macrolide antibiotic erythromycin, and it has been shown to play a critical role in the biological activity of the drug. Desosamine is added to the parent aglycone via the action of a glycosyltransferase that utilizes dTDP-desosamine as its substrate. Six enzymes are required for the biosynthesis of dTDP-desosamine in *Streptomyces venezuelae*, with the last step catalyzed by DesVI, an *N*,*N*-dimethyltransferase. Here we describe the X-ray crystal structure determined to 2.0 Å resolution of DesVI complexed with *S*-adenosylmethionine (SAM) and the substrate analogue UDP-benzene. Each subunit of the DesVI dimer contains a seven-stranded mixed β-sheet flanked on either side by α-helices. In addition to this major tertiary structural element, there is a four-stranded antiparallel β-sheet that provides the platform necessary for subunit−subunit assembly. On the basis of the UDP-benzene binding mode, the DesVI substrate, dTDP-3-(methylamino)-3,4,6-trideoxyglucose, has been modeled into the active site. This model places the C-6′ methyl group of the sugar into a hydrophobic patch that is well-conserved among putative nucleotide-linked sugar dimethyltransferases. It is formed by Trp 140, Met 178, and Ile 200. The sugar C-2′ hydroxyl sits near Tyr 14, and its C-3′ amino group is properly positioned for direct in-line attack of the cofactor's reactive methyl group. While methyltransferases that catalyze single alkylations at carbons, oxygens, sulfurs, and nitrogens have been well characterized, little is known regarding enzymes capable of N,N-dimethylation reactions. As such, the ternary structure of DesVI reported here serves as a structural paradigm for a new family of dimethyltransferases that function on nucleotide-linked sugars.

Macrolide antibiotics constitute an old and well-established class of antimicrobial agents first introduced into the clinical setting more than 50 years ago (*1*). These types of therapeutics contain large lactone rings, which are typically 14-, 15-, or 16-membered. One of the oldest of these is erythromycin, a complex molecule consisting of a 14-membered macrocyclic ring and two unusual sugars, L-cladinose and D-desosamine[1] (*2*). These sugars are appended to the macrolide scaffold via the action of glycosyltransferases which utilize nucleotide-linked sugars as their substrates (*3*). In recent years, it has been demonstrated that unusual sugars such as desosamine or cladinose provide or enhance the pharmacological properties of the macrolide antibiotics to which they are attached (*4*). The desosamine moiety of erythromycin, for example, increases the binding affinity of the drug for the 50S bacterial ribosome subunit (*5*). Removal of the desosamine unit, or even a slight modification of the sugar thereof, greatly reduces the bactericidal activities of the drug (*6, 7*). Because of the biological importance of unusual sugars to natural compounds, the concept of "glycodiversification" has been championed within the past few years whereby sugars and/or the glycosylation patterns of the macrolide scaffolds are altered as a means of producing new and potentially important therapeutics (*8–10*).

As shown in Scheme 1, six enzymes are thought to be required for the biosynthesis of dTDP-desosamine (*11*). The first two steps, namely, the attachment of α-D-glucose 1-phosphate to dTMP and the subsequent removal of the C-6′ hydroxyl group and the oxidation of the C-4′ hydroxyl group, are typical for most pathways leading to the formation of 3,6-dideoxyhexoses or 2,3(4),6-trideoxyhexoses. DesIII and DesIV catalyze these reactions, respectively. The next two steps in the pathway, which are catalyzed by DesI and DesII,

[†] This research was supported by NIH Grant DK47814 to H.M.H.

[‡] X-ray coordinates have been deposited in the Research Collaboratory for Structural Bioinformatics, Rutgers University, New Brunswick, N. J. (PDB entry 3BXO).

* To whom correspondence should be addressed. E-mail: Hazel_Holden@biochem.wisc.edu. Fax: (608) 262-1319. Phone: (608) 262-4988.

[1] Abbreviations: D-desosamine, 3-(dimethylamino)-3,4,6-trideoxyglucose; DMSO, dimethyl sulfoxide; HEPES, *N*-(2-hydroxyethyl)piperazine-*N*′-2-ethanesulfonic acid; HEPPS, *N*-(2-hydroxyethyl)piperazine-*N*′-3-propanesulfonic acid; IPTG, isopropyl β-D-1-thiogalactopyranoside; MAD, multiple-wavelength anomalous dispersion; MES, 2-(*N*-morpholino)ethanesulfonic acid; Ni-NTA, nickel-nitrilotriacetic acid; PCR, polymerase chain reaction; PLP, pyridoxal 5′-phosphate; dTDP, 2-deoxythymidine diphosphate; rTEV, recombinant tobacco etch virus; SAH, *S*-adenosylhomocysteine; SAM, *S*-adenosylmethionine; UDP-benzene, uridine diphosphobenzene.

10.1021/bi800063j CCC: $40.75
Published on Web 03/08/2008

Scheme 1

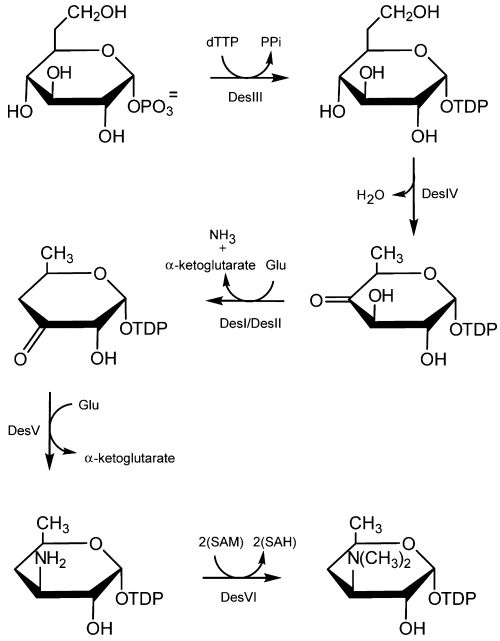

respectively, lead to the loss of the sugar C-4′ hydroxyl group and the oxidation of the C-3′ hydroxyl. The penultimate step in dTDP-desosamine biosynthesis is catalyzed by DesV, a PLP-dependent transaminase (Scheme 1).

The focus of this investigation is DesVI, which catalyzes the last step in dTDP-desosamine biosynthesis. It is an unusual *N*,*N*-dimethyltransferase that employs *S*-adenosylmethionine (SAM) as its cofactor. Previous studies have demonstrated that the homodimeric enzyme catalyzes N,N-dimethylation of the sugar C-3′ amino group in a stepwise manner with SAM binding first to the enzyme followed by the sugar substrate (*12*). In addition, experiments indicate that upon the first N-methylation reaction, both the monomethylated intermediate and *S*-adenosylhomocysteine (SAH) are released from the active site of the enzyme (*12*). Subsequent binding of another SAM cofactor and the monomethylated intermediate leads to the final product shown in Scheme 1.

Methylation is a common theme in biology, but most methyltransferases characterized to date catalyze single alkylations at carbons, oxygens, sulfurs, or nitrogens. Indeed, SAM-dependent methyltransferases that modify DNA, RNA, histones, and other proteins have been well studied and reviewed (*13, 14*). Much less is known regarding dimethylation reactions, however. While the structure of KsgA, a universally conserved rRNA adenine dimethyltransferase, has recently been reported (*15*), there is still a paucity of structural information regarding *N*,*N*-dimethyltransferases, and, in particular, those that utilize nucleotide-linked sugars as their substrates.

For the X-ray diffraction analysis presented here, we crystallized DesVI from *Streptomyces venezuelae* in the presence of *S*-adenosylmethionine and the substrate analogue UDP-benzene. The structure shows that DesVI belongs to the class I methyltransferase family (*16*). Members belonging to this family contain a core fold composed of a seven-stranded mixed β-sheet flanked on either side by α-helices. In addition to the core fold, DesVI contains a four-stranded antiparallel β-sheet that is intimately involved in subunit−subunit interactions. On the basis of the observed UDP-benzene binding position, we propose a model for the manner in which the natural substrate, dTDP-3-(methylamino)-3,4,6-trideoxyglucose, is accommodated within the DesVI active site cleft.

Carbohydrate moieties found in natural products are often essential for the biological activity of the parent compounds to which they are attached. This is most likely due to their three-dimensional structures that allow for the precise placement of functional groups, which can alter the solubility, charge distribution, and/or specific binding properties of the parent compound. One key advantage of using carbohydrates in antibiotic design is that they provide a stable framework upon which to build new molecules with altered biological specificities. Unusual carbohydrates are, however, notoriously difficult to synthesize in vitro. Nevertheless, microorganisms have developed an impressive arsenal of enzymes that circumvent many of these difficulties. Thus, by utilizing the catalysts already present in nature, many unique carbohydrate modifications can be made in vitro and in vivo via the judicious use of site-directed mutant proteins. The model of DesVI described here represents the first structural report of a sugar dimethyltransferase and thus provides a three-dimensional foundation upon which to expand its catalytic capabilities toward producing sugars not heretofore encountered in nature. In addition, the structure serves as a paradigm for a new family of small molecule *N*,*N*-dimethyltransferases.

EXPERIMENTAL PROCEDURES

Cloning of the Gene Encoding DesVI. Genomic DNA was isolated from *S. venezuelae* as previously reported (*17*). The gene encoding DesVI was amplified from genomic DNA via PCR, after which the PCR products were ligated into the pGEM (Promega) vector for screening. The DesVI gene was excised from the pGEM vector with NdeI and XhoI (Promega) and ligated into a pET28b(+) vector (Novagen) for subsequent expression of DesVI with an rTEV cleavable N-terminal polyhistidine tag (*18*). The resulting pET28-DesVI plasmid was utilized for transformation of *Escherichia coli* Rosetta DE3 cells (Novagen).

Protein Expression and Purification. Wild-type DesVI was expressed using the transformed *E. coli* Rosetta DE3 cells which were grown in LB medium. For expression of selenomethionine-labeled protein, cells were first grown in M9 medium containing 5 mg/L vitamin B_1 to an OD_{600} of 0.8 cm^{-1} at 37 °C. Subsequently, the medium was supplemented with 50 mg/L leucine, isoleucine, valine, and selenomethionine and 100 mg/L lysine, threonine, and phenylalanine (*17*). In the growths for both the wild-type and selenomethionine-labeled protein, the cells were cooled on ice before the addition of 1 mM IPTG. Incubation was continued overnight at 16 °C.

Cells were harvested by centrifugation and flash-frozen in liquid nitrogen. Sonication was used to disrupt the cells at 0 °C in 50 mM sodium phosphate, 10 mM imidazole, and 150 mM NaCl (pH 8.0), and cellular debris was removed by centrifugation. The supernatant was passed through a Ni-NTA column (Qiagen), and bound protein was eluted with a 10 to 300 mM linear gradient of imidazole [50 mM sodium phosphate and 150 mM NaCl (pH 8.0)]. The polyhistidine tag on wild-type DesVI was cleaved with rTEV, and the

Table 1: X-ray Data Collection Statistics

	peak[a]	inflection[a]	remote[a]	ternary complex[b]
wavelength (Å)	0.97907	0.97924	0.96441	1.54178
resolution limits (Å)	50–2.0 (2.07–2.0)[c]	50–2.0 (2.07–2.0)	50–2.0 (2.07–2.0)	30–2.0 (2.1–2.0)
no. of independent reflections	41001 (3760)	41001 (3716)	41181 (4031)	36362 (11559)
completeness (%)	99.1 (92.3)	99.0 (91.6)	99.6 (99.0)	89.8 (76.5)
redundancy	6.5 (5.6)	6.5 (5.6)	6.5 (6.1)	2.7 (1.9)
avg I/avg $\sigma(I)$	38.0 (11.1)	37.2 (10.3)	39.3 (12.9)	9.4 (2.6)
R_{sym}[d] (%)	6.6 (12.8)	6.3 (13.2)	5.2 (10.8)	8.4 (25.4)

[a] Refers to X-ray data collected for MAD phasing. [b] Refers to X-ray data collected for least-squares refinement of the ternary complex. [c] Statistics for the highest-resolution bin. [d] $R_{sym} = (\sum|I - \bar{I}|/\sum I) \times 100$.

reaction mixture was purified by Ni-NTA column chromatography. Both wild-type and selenomethionine-labeled DesVI were concentrated by ultrafiltration and dialyzed against a storage buffer containing 10 mM HEPES and 150 mM NaCl (pH 7.5). For the wild-type protein, the yield was 1.2 g per 12 L of medium, whereas for the selenomethionine-labeled protein, the yield was slightly lower at 600 mg per 12 L of medium.

Crystallization of DesVI. Crystallization conditions for wild-type and selenomethionine-labeled DesVI were initially surveyed by the hanging drop method of vapor diffusion with a sparse matrix screen developed in the laboratory. Diffraction quality crystals of the selenomethionine-labeled DesVI were subsequently grown via the hanging drop method by mixing 10 μL of DesVI (30 mg/mL in storage buffer supplemented with 30 mM SAM) with 10 μL of a precipitant solution containing 2.0 M ammonium sulfate, 8% DMSO, and 100 mM HEPPS (pH 8.0). These crystals grew to maximum dimensions of 1.0 mm × 0.4 mm × 0.2 mm after 2 weeks at 4 °C and belonged to space group $P2_12_12$ with one dimer in the asymmetric unit and the following unit cell dimensions: $a = 61.7$ Å, $b = 133.1$ Å, and $c = 72.9$ Å.

Wild-type DesVI crystals were grown via the hanging drop method of vapor diffusion by mixing 3 μL of protein (17 mg/mL in storage buffer containing 30 mM SAM and 10 mM UDP-benzene) with 3 μL of a precipitant solution containing 20% poly(ethylene glycol) 5000 monomethyl ether and 100 mM MES (pH 6.0). These crystals grew to maximum dimensions of ~0.7 mm × 0.7 mm × 0.05 mm after 2 weeks at 4 °C. They belonged to space group $P2_1$ with one dimer per asymmetric unit and the following unit cell dimensions: $a = 46.2$ Å, $b = 56.1$ Å, $c = 116.5$ Å, and $\beta = 92.5°$.

Structural Analysis of DesVI. For X-ray data collection, the selenomethionine-labeled DesVI crystals were transferred into a synthetic mother liquor containing 2.0 M ammonium sulfate, 75 mM NaCl, 20 mM SAM, and 100 mM HEPPS (pH 8.0). They were then acclimated via four incremental transfers to a cryoprotectant solution containing 2.0 M ammonium sulfate, 200 mM NaCl, 40 mM SAM, 25% sucrose, and 100 mM HEPPS (pH 8.0). X-ray data sets from a single crystal were collected to 2.0 Å resolution at the Advanced Photon Source, Argonne National Laboratory, Structural Biology Center, beamline 19-BM on a 3 × 3 tiled "SBC3" CCD detector. These data were processed with HKL2000 (*19*) and internally scaled with SCALEPACK (*19*). Relevant X-ray data collection statistics are given in Table 1.

The structure of selenomethione-labeled DesVI was determined by MAD phasing using SOLVE to locate the selenium positions and to calculate protein phases (*20*). The initial protein phases were further improved by both molecular averaging and solvent flattening with RESOLVE (*21*). A model of DesVI was constructed with ARP/wARP (*22*) and manually adjusted using TURBO (*23*).

For the crystallographic analysis of wild-type DesVI complexed with SAM and UDP-benzene, an X-ray data set was collected to 2.0 Å resolution using a Bruker AXS Platinum 135 CCD detector equipped with Montel optics. The X-ray source was Cu Kα radiation from a Rigaku RU200 X-ray generator operated at 50 kV and 90 mA. The crystal utilized for X-ray data collection was first transferred to a synthetic mother liquor containing 18% poly(ethylene glycol) 5000 monomethyl ether, 30 mM SAM, 10 mM UDP-benzene, and 100 mM MES (pH 6.0) and then, by four incremental transfers, to a cryoprotectant solution containing 19% poly(ethylene glycol) 5000 monomethyl ether, 30 mM SAM, 10 mM UDP-benzene, 20% ethylene glycol, and 100 mM MES (pH 6.0). These X-ray data were processed with SAINT [Bruker (2003) *SAINT*, version V7.06A, Bruker AXS Inc., Madison, WI] and internally scaled with SADABS [Sheldrick, G. M. (2002) *SADABS*, version 2005/1, Bruker AXS Inc., Madison, WI]. The overall Wilson B-factor for the X-ray data set was 8.8 Å^2. Initial protein phases were generated by molecular replacement with PHASER (*24*) and using the partially refined model of the selenomethionine-labeled DesVI as a search probe. Alternate cycles of least-squares refinement with TNT (*25*) and manual adjustment with Coot (*26*) reduced the overall R-factor to 16.9% for all measured X-ray data from 30 to 2.0 Å. Noncrystallographic restraints were not used in the refinement. Peaks of electron density in maps calculated with $F_o - F_c$ coefficients were considered to be water molecules if they were within ~3.6 Å of potential hydrogen-bonding groups. Relevant refinement statistics are given in Table 2.

RESULTS AND DISCUSSION

Overall Structure of DesVI. The crystals of wild-type DesVI in complex with SAM and UDP-benzene used for this structural analysis contained one homodimer in the asymmetric unit. Electron density for both subunits was continuous from Tyr 2 to the C-terminal residue, Ala 237. The overall geometry of the DesVI model is excellent with 93.6 and 6.4% of the backbone φ and ψ angles lying within the core and allowed regions of the Ramachandran plot, respectively. The two subunits of the dimer superimpose with a root-mean-square deviation of 0.18 Å, and thus for the sake of simplicity, the following discussion refers only to subunit 1 in the X-ray coordinate file unless otherwise noted.

Table 2: Least-Squares Refinement Statistics

resolution limits (Å)	30–2.0
R-factor[a] (overall) (%)/no. of reflections	16.9/36362
R-factor (working) (%)/no. of reflections	16.5/32744
R-factor (free) (%)/no. of reflections	25.4/3618
no. of protein atoms[b]	3718
no. of heteroatoms[c]	664
average *B*-values (Å^2)	
protein atoms	17.0
ligands	16.5
solvents	28.4
weighted rms deviations from ideality	
bond lengths (Å)	0.010
bond angles (deg)	2.0
trigonal planes (Å)	0.007
general planes (Å)	0.007
torsional angles[d] (deg)	17.6

[a] *R*-factor = $(\sum|F_o - F_c|/\sum|F_o|) \times 100$, where F_o is the observed structure-factor amplitude and F_c is the calculated structure-factor amplitude. [b] These include multiple conformations for Arg 33 and Glu 172 in subunit 1 and Thr 74, Arg 157, Glu 172, and Arg 218 in subunit 2. [c] These include two SAM cofactors, two UDP-benzene molecules, 544 waters, and one ethylene glycol. [d] The torsional angles were not restrained during the refinement.

Shown in Figure 1a is a ribbon representation of the DesVI dimer which has overall dimensions of ~57 Å × 38 Å × 98 Å. The subunit−subunit interface is formed by a four-stranded antiparallel β-sheet from one subunit (β-strands 6−9) abutting the symmetry-related β-sheet from the second subunit leading to a modest buried surface area of 825 Å^2 per subunit. The dimer interface is quite hydrophilic in character with, strikingly, no side chain aromatic stacking interactions. There is one prominent hydrogen bond between the side chain of His 168 in subunit 1 and the backbone amide nitrogen of Gly 188 in subunit 2 (and, equivalently, His 168 in subunit 2 and Gly 188 in subunit 1). The active sites in the dimer are separated by ~38 Å.

The individual subunits contain 11 β-strands and seven α-helices and are distinctly bilobal in appearance (Figure 1b). The active sites are wedged between the two lobes. As can be seen in panels b and c of Figure 1, the major tertiary structural motif of the subunit is a seven-stranded mixed β-sheet with β-strands 1−5 and 10 running parallel. This motif differs from the canonical "SAM methyltransferase fold" primarily by an insertion after β-strand 5 which results in the four-stranded antiparallel β-sheet involved in the above-mentioned subunit−subunit interactions (*27*). A second major embellishment to the core methyltransferase fold is the N-terminal helix, which lies between the N- and C-terminal domains. A search with the Dali server (*28*) reveals that the closest structural relative to DesVI is rat liver glycine *N*-methyltransferase which functions as a tetramer and also has an extended N-terminal region (*29, 30*). Whereas there is little overall detectable amino acid sequence homology between DesVI and rat liver glycine *N*-methyltransferase, the individual subunits for the two enzymes superimpose with a root-mean-square deviation of 1.9 Å for 201 structurally equivalent α-carbons. The active sites for these two enzymes, while similar with regard to SAM positioning, are dissimilar with respect to their substrate binding pockets.

Electron densities corresponding to SAM and UDP-benzene are presented in Figure 2a. These two ligands bind in the active site pocket such that the reactive methyl group of SAM is located within ~3.7 Å of C-4′ of UDP-benzene. Whereas the electron density corresponding to SAM is very well-ordered as is the nucleotide portion of the substrate analogue, the electron density for the benzene ring is somewhat weaker, suggesting a higher degree of mobility. A close-up stereoview of the DesVI active site is displayed in Figure 2b. The uracil ring of UDP-benzene is flanked on either side by Trp 141 and Trp 150 and lies within hydrogen bonding distance of the carbonyl oxygen of Thr 145. The uracil ribose adopts the C_2'-*endo* pucker with the C-2 and C-3 hydroxyl groups participating in hydrogen bonds with the carbonyl oxygen of Ala 147 and O_γ of Ser 169, respectively. Three arginines (17, 165, and 229) form electrostatic interactions with the phosphoryl groups of the substrate analogue. In addition, the side chains of Tyr 14, Ser 152, and Ser 167 and two water molecules serve to anchor the UDP-benzene into the active site pocket. A notable T-shaped stacking interaction occurs between the benzene ring and the side chain of Phe 106.

The adenine ring of SAM is held in the active site via hydrogen bonds with the carboxylate group of Asp 89, the backbone amide nitrogen of Met 90, and an ordered water molecule. As observed for UDP-benzene, the adenine ribose adopts the C_2'-*endo* pucker. Glu 67 bridges the C-2 and C-3 hydroxyl groups of the sugar. An additional hydrogen bond occurs between the ribose C-2 hydroxyl group and a water molecule. Tyr 21 and a water molecule interact with the α-carboxylate of SAM, whereas the carbonyl oxygens of Ala 46 and Met 105 and two water molecules hold the α-amino group of the cofactor in place. Ala 46 belongs to the characteristic signature sequence termed motif I in many SAM-dependent methyltransferases. It is a nine-residue block containing the sequence (V/I/L)-(L/V)-(D/E)-(V/I)-G-(G/C)-G-(T/P)-G (*31*). In DesVI, this sequence is Leu 42-Leu 43-Asp 44-Val 45-Ala 46-Cys 47-Gly 48-Thr 49-Gly 50, and it encompasses the loop leading from the first β-strand to the third α-helix of the subunit.

One question that might be raised is whether UDP-benzene is an appropriate substrate analogue for the natural DesVI substrate, dTDP-3-amino-3,4,6-trideoxyglucose, and, in particular, whether the aromatic group of the analogue mimics carbohydrate binding. While substrate analogues are never perfect, there is ample evidence in the literature, particularly in the structural studies of UDP-galactose 4-epimerase, that UDP-benzene is a good mimic for a nucleotide-linked sugar (*32*). On the basis of the observed binding of UDP-benzene to DesVI, we have built a model of the monomethylated form of dTDP-3-amino-3,4,6-trideoxyglucose into the active site of the enzyme as displayed in Figure 2c. This orientation of the substrate places its C-6′ methyl group into a hydrophobic pocket defined by Trp 140, Met 178, and Ile 200. DesVI demonstrates significant homology to the deduced amino acid sequences of *tylM1* from *Streptomyces fradiae*, *eryCVI* from *Saccharopolyspora erythraea*, *snoX* from *Streptomyces nogalater*, *rdmD* from *Streptomyces purpurascens*, and *srmX* from *Streptomyces ambofaciens*, and it has been proposed that these genes encode *N*,*N*-dimethyltransferases (*12*). On the basis of an alignment of the deduced amino acid sequences for the above-mentioned-proteins, it should be noted that Trp 140 is absolutely conserved, Met 178 is conserved or replaced with an isoleucine, and Ile 200 is conserved or replaced with a leucine. Hence, the character of this hydrophobic patch is retained, lending support to our model which places the C-6′ methyl group in the position indicated

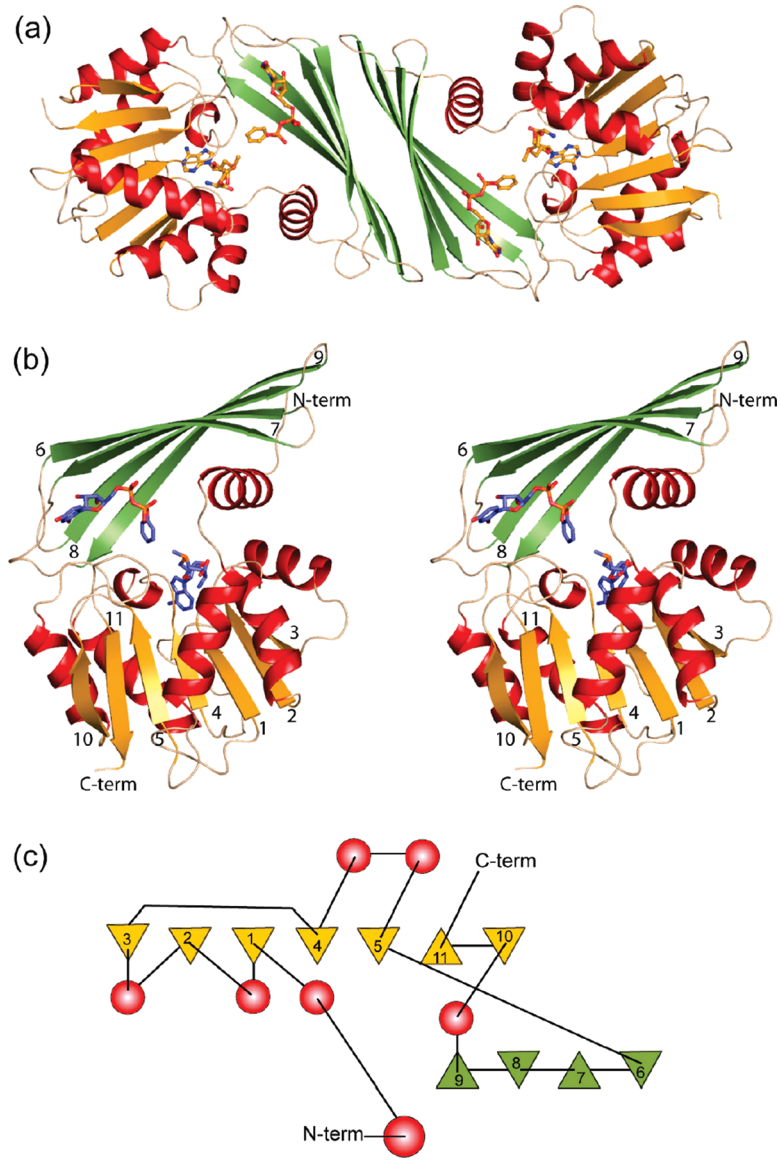

FIGURE 1: Structure of DesVI. (a) Ribbon representation of the DesVI dimer. The subunit−subunit interface is formed by two layers of antiparallel β-sheet highlighted in green. The stick representations correspond to the bound ligands, SAM and UDP-benzene. (b) Stereoview of the subunit architecture. The active site is wedged between the domains and is bounded on one side by the N-terminal α-helix and on the other by regions of loops and helices that connect β-strands 4 to 5, 5 to 6, and 9 to 10. (c) Topology of the subunit. Circles and triangles represent α-helices and β-strands, respectively. This topology drawing was prepared with TOPS (*35*). All other figures were prepared with PyMol (*36*).

in Figure 2c. The sugar C-2′ hydroxyl group in our model lies within hydrogen bonding distance of Tyr 14, and we suggest that this residue plays a role in substrate positioning. It is typically a tyrosine or histidine in the other putative sugar *N*,*N*-dimethyltransferases. Catalysis by methyltransferases is known to proceed by an S_N2 displacement reaction with inversion of the stereochemistry about the methyl group of the cofactor (*33*). In our proposed model, the sugar C-3′ amino nitrogen is situated ~2.7 Å from and in line to attack the reactive methyl group of SAM.

The active site of DesVI is designed to bind two different sugar substrates, namely, dTDP-3-amino-3,4,6-trideoxyglucose and 3-(methylamino)-3,4,6-trideoxyglucose. According to the model presented in Figure 2c, the monomethylated substrate is accommodated in the active site pocket with its 3-methylamino group projecting into a pocket delineated by the side chains of Phe 106, Trp 140, and Arg 229. The guanidinium group of Arg 229 is involved in electrostatic interactions with the β-phosphoryl group of the dTDP-linked sugar, and consequently, the putative 3-methylamino group binding pocket is reasonably hydrophobic. Importantly, there is enough room in the active site for DesVI to accept the larger sugar substrate. If the size of the DesVI active site is decreased via site-directed mutagenesis, it should be possible to produce the monomethylated product exclusively. This work is in progress.

The use of nucleotide-linked deoxysugars as tools for altering the glycosylation patterns of aglycone rings represents a powerful approach for the design of new therapeutics (*10*, *34*). By understanding the structures of the enzymes involved in the biosynthesis of unusual di- and trideoxysugars, we should be able to prepare site-directed mutant proteins with altered substrate specificities yielding nucleotide-linked sugars not normally encountered in nature. The structure of DesVI presented here provides one such molecular foundation for unique sugar design.

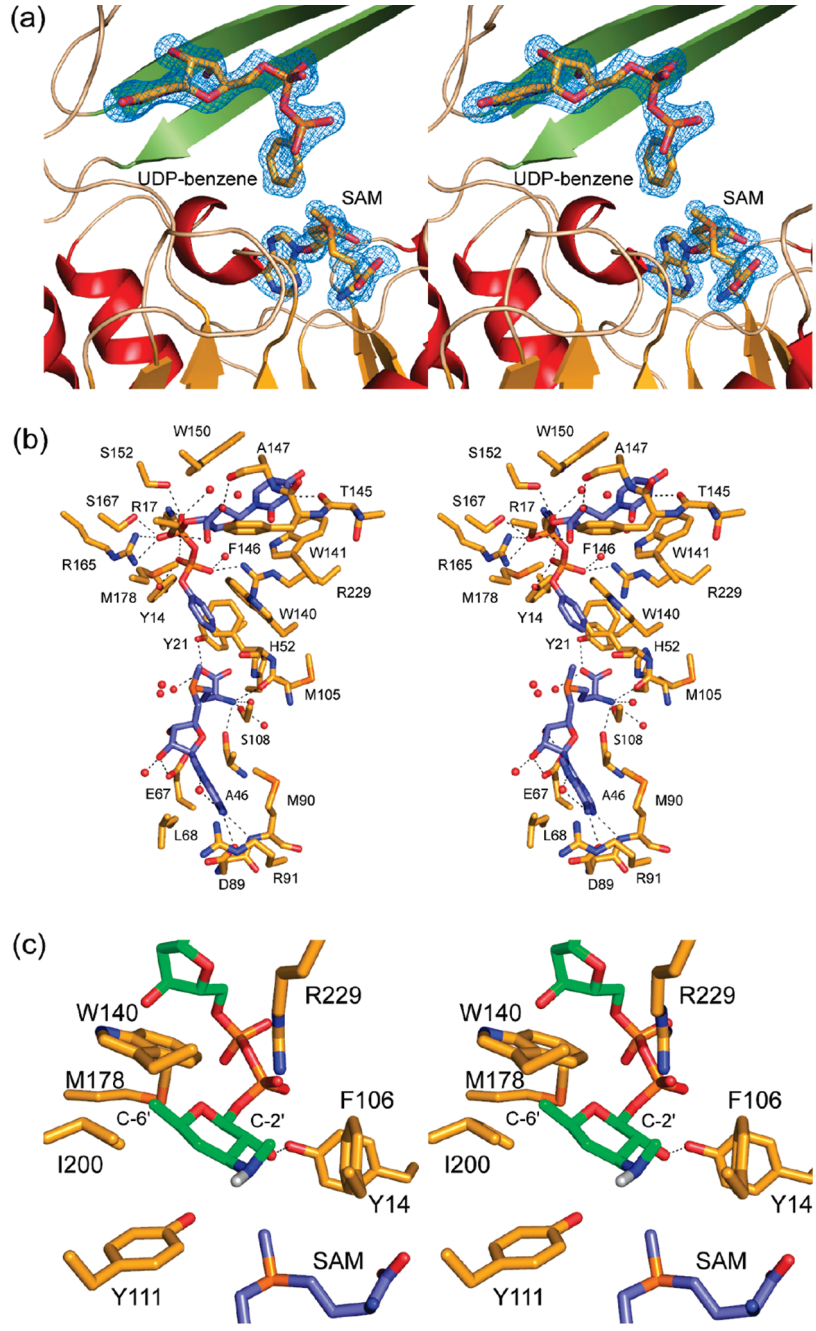

FIGURE 2: Active site of DesVI. (a) Electron density corresponding to the bound SAM and UDP-benzene molecules. The map was calculated with coefficients of the form $F_o - F_c$, where F_o is the native structure-factor amplitude and F_c the calculated structure-factor amplitude with atoms corresponding to bound ligands excluded from the calculation. The map was contoured at 3σ. (b) Close-up stereoview of the active site. Those residues lying within 3.5 Å of the bound ligands are shown. For the sake of clarity, Phe 106 and Ser 169 are shown but not labeled. Possible hydrogen bonds are represented by dashed lines. (c) Possible binding mode for dTDP-3-(methylamino)-3,4,6-trideoxyglucose. Only those residues immediately adjacent to the hexose of the substrate and the reactive methyl group of SAM are shown. The sugar moiety is highlighted in green, whereas SAM is displayed with slate bonds. The hydrogen attached to the 3-methylamino group is colored white.

ACKNOWLEDGMENT

We gratefully acknowledge the helpful discussions of Mr. Paul D. Cook and Drs. James B. Thoden and W. W. Cleland. We thank Mr. Nate Bruender for help with the model refinement.

REFERENCES

1. Goldman, R. C., and Scaglione, F. (2004) The macrolide-bacterium interaction and its biological basis. *Curr. Drug Targets Infect. Disord. 4*, 241–260.
2. Katz, L., and Donadio, S. (1995) *Genetics and Biochemistry of Antibiotic Production*, Butterworth-Heinemann Ltd., Boston, MA.
3. Trefzer, A., Salas, J. A., and Bechthold, A. (1999) Genes and enzymes involved in deoxysugar biosynthesis in bacteria. *Nat. Prod. Rep. 16*, 283–299.
4. Weymouth-Wilson, A. C. (1997) The role of carbohydrates in biologically active natural products. *Nat. Prod. Rep. 14*, 99–110.
5. Schlunzen, F., Zarivach, R., Harms, J., Bashan, A., Tocilj, A., Albrecht, R., Yonath, A., and Franceschi, F. (2001) Structural basis for the interaction of antibiotics with the peptidyl transferase centre in eubacteria. *Nature 413*, 814–821.
6. Thorson, J. S., and Vogt, T. (2002) *Glycosylated Natural Products*, Wiley-VCH, Weinheim, Germany.

7. Iacoviello, V. R., and Zinner, S. H. (2002) *Macrolide Antibiotics*, Berkhäuser, Basel, Switzerland.
8. Yang, J., Hoffmeister, D., Liu, L., Fu, X., and Thorson, J. S. (2004) Natural product glyorandomization. *Bioorg. Med. Chem. 12*, 1577–1584.
9. Blanchard, S., and Thorson, J. S. (2006) Enzymatic tools for engineering natural product glycosylation. *Curr. Opin. Chem. Biol. 10*, 263–271.
10. Thibodeaux, C. J., Melancon, C. E., and Liu, H. W. (2007) Unusual sugar biosynthesis and natural product glycodiversification. *Nature 446*, 1008–1016.
11. Borisova, S. A., Zhang, C., Takahashi, H., Zhang, H., Wong, A. W., Thorson, J. S., and Liu, H. W. (2006) Substrate specificity of the macrolide-glycosylating enzyme pair DesVII/DesVIII: Opportunities, limitations, and mechanistic hypotheses. *Angew. Chem., Int. Ed. 45*, 2748–2753.
12. Chen, H., Yamase, H., Murakami, K., Chang, C. W., Zhao, L., Zhao, Z., and Liu, H. W. (2002) Expression, purification, and characterization of two N,N-dimethyltransferases, tylM1 and desVI, involved in the biosynthesis of mycaminose and desosamine. *Biochemistry 41*, 9165–9183.
13. Fontecave, M., Atta, M., and Mulliez, E. (2004) S-Adenosylmethionine: Nothing goes to waste. *Trends Biochem. Sci. 29*, 243–249.
14. Loenen, W. A. (2006) S-Adenosylmethionine: Jack of all trades and master of everything? *Biochem. Soc. Trans. 34*, 330–333.
15. O'Farrell, H. C., Scarsdale, J. N., and Rife, J. P. (2004) Crystal structure of KsgA, a universally conserved rRNA adenine dimethyltransferase in *Escherichia coli*. *J. Mol. Biol. 339*, 337–353.
16. Schubert, H. L., Blumenthal, R. M., and Cheng, X. (2003) Many paths to methyltransfer: A chronicle of convergence. *Trends Biochem. Sci. 28*, 329–335.
17. Burgie, E. S., Thoden, J. B., and Holden, H. M. (2007) Molecular architecture of DesV from *Streptomyces venezuelae*: A PLP-dependent transaminase involved in the biosynthesis of the unusual sugar desosamine. *Protein Sci. 16*, 887–896.
18. Thoden, J. B., and Holden, H. M. (2005) The molecular architecture of human *N*-acetylgalactosamine kinase. *J. Biol. Chem. 280*, 32784–32791.
19. Otwinowski, Z., and Minor, W. (1997) Processing of X-ray diffraction data collected in oscillation mode. *Methods Enzymol. 276*, 307–326.
20. Terwilliger, T. C., and Berendzen, J. (1999) Automated MAD and MIR structure solution. *Acta Crystallogr. D55* (Part 4), 849–861.
21. Terwilliger, T. C. (2000) Maximum-likelihood density modification. *Acta Crystallogr. D56* (Part 8), 965–972.
22. Lamzin, V. S., Perrakis, A., and Wilson, K. S. (2001) *The ARP/wARP suite for automated construction and refinement of protein models*, Vol. F, Kluwer Academic Publishers, Dordrecht, The Netherlands.
23. Roussel, A., Fontecilla-Camps, J. C., and Cambillau, C. (1990) in XV IUCr Congress, pp 66–67, Bordeaux, France.
24. McCoy, A. J., Grosse-Kunstleve, R. W., Storoni, L. C., and Read, R. J. (2005) Likelihood-enhanced fast translation functions. *Acta Crystallogr. D61*, 458–464.
25. Tronrud, D. E., Ten Eyck, L. F., and Matthews, B. W. (1987) An efficient general-purpose least-squares refinement program for macromolecular structures. *Acta Crystallogr. A43*, 489–501.
26. Emsley, P., and Cowtan, K. (2004) Coot: Model-building tools for molecular graphics. *Acta Crystallogr. D60*, 2126–2132.
27. Martin, J. L., and McMillan, F. M. (2002) SAM (dependent) I AM: The S-adenosylmethionine-dependent methyltransferase fold. *Curr. Opin. Struct. Biol. 12*, 783–793.
28. Holm, L., and Sander, C. (1996) Mapping the protein universe. *Science 273*, 595–603.
29. Fu, Z., Hu, Y., Konishi, K., Takata, Y., Ogawa, H., Gomi, T., Fujioka, M., and Takusagawa, F. (1996) Crystal structure of glycine *N*-methyltransferase from rat liver. *Biochemistry 35*, 11985–11993.
30. Takata, Y., Huang, Y., Komoto, J., Yamada, T., Konishi, K., Ogawa, H., Gomi, T., Fujioka, M., and Takusagawa, F. (2003) Catalytic mechanism of glycine *N*-methyltransferase. *Biochemistry 42*, 8394–8402.
31. Kagan, R. M., and Clarke, S. (1994) Widespread occurrence of three sequence motifs in diverse *S*-adenosylmethionine-dependent methyltransferases suggests a common structure for these enzymes. *Arch. Biochem. Biophys. 310*, 417–427.
32. Thoden, J. B., Frey, P. A., and Holden, H. M. (1996) High-resolution X-ray structure of UDP-galactose 4-epimerase complexed with UDP-phenol. *Protein Sci. 5*, 2149–2161.
33. Bugg, T. (1997) *An Introduction to Enzyme and Coenzyme Chemistry*, Blackwell Science Ltd., Oxford, U.K.
34. Rupprath, C., Schumacher, T., and Elling, L. (2005) Nucleotide deoxysugars: Essential tools for the glycosylation engineering of novel bioactive compounds. *Curr. Med. Chem. 12*, 1637–1675.
35. Michalopoulos, I., Torrance, G. M., Gilbert, D. R., and Westhead, D. R. (2004) TOPS: An enhanced database of protein structural topology. *Nucleic Acids Res. 32*, D251–D254.
36. DeLano, W. L. (2002) *The PyMOL Molecular Graphics System*, DeLano Scientific, San Carlos, CA.

BI800063J